2D ANALYSIS FOR COMPUTING SUPERSONIC AND SUBSONIC FLOW FIELD BY USING SCHLIEREN LIGHT

التحليل ثنائى الأبعاد لحساب مجال السريان فوق و دون سرعه الصوت باستخدام ضوء شليرن

Nabil H. Mostafa
Mechanical Power Department, College of Engineering
Zagazig University, Zagazig, 44519, Egypt.
Tel: +[20] 50 2334688 Fax: +[20] 50 2331911
E-mail: nmostafa@egyptnetwork.com

الخلاصة:

يتناول هذا البحث طريقه جديده لحساب توزيع السرعات فى مجال السريان لمناطق فوق و دون سرعه الصوت و أيضا مناطق تمدد المائع و ذلك بتحليل ضوء شليرن. و قد ثبت دقتها بمقارنة تلك النتائج بالنتائج الحسابيه ثنائيه الأبعاد. حيث أن ادخال مجسات قياس تجريبيه في مناطق موجة التصادم وما يصاحبها فى مجال السريان صعب للغاية لتغير الضغط و الكثافة بمعدلات عالية و التى تؤدى الى أنكسار الضوء. إن شدة ضوء شليرن دالة في كثافة الوسط و التى هي بدورها دالة في مسار الشعاع الضوني. إن شدة الضوء في كل وحدة ضونية (pixel) قد حدد بتحليل الصورة. و قد إستنبطت مجموعه من المعادلات لتربط نسبه شده الضوء في صوره شليرن مع رقم ماخ في كل عنصر. هذه الدوال قد طبقت على صوره فى نطقه موجه تصادم حول اسطوانه ذات مقدمه نصف كرويه لرقم ماخ ١,٩٦ .

و للتأكد من دقه تلك النتائج التحليليه المستنتجه من هذه الطريقه فقد إستعملت معادلات نافير استوكس مع معادلات بقاء الطاقه لنمذجه سريان المائع فى نفس الظروف السابقه. حيث تم تمثيل المعادلات الحاكمه على شبكه منشأه باستخدام نظام فرق الاختلاف المضاد للاتجاه. وقد أظهرت النتائج تطابق الدراسه النظريه مع تلك المستنتجه من التحليل الضوئى بفارق لا يتعدى ٣% حيث الحصول على منطقة بدء السريان ومنطقة موجة التصادم و منطقة السريان دون الصوتي و كذلك منطقة التمدد. إن هذا الفارق قد يكون نتج عن التشوه الموجود فى الصوره. وهذا التشويه ممكن استبعاده باستقبال الضوء مباشرة على كاميرا رقميه. و قد أظهرت النتائج أن هذه الطريقة يمكن تطبيقها في كلا الجزئيين المضيء و الداكن من صوره شليرن مع تصحيح الترحيل الموجى فى الجزء المظلم. هذه الطريقة الضوئية لها كافة المميزات الخاصة بوسائل القياس الضونية مثل عدم تشوه حركه المائع و حساسية متابعة التغيرات اللحظية.

ABSTRACT

A new 2D analysis of light for computing the Mach number distribution in a flow field from Schlieren images taken across the shock wave and expansion zone is proposed and verified by a 2D numerical computation. Specially, inserting experimental measuring sensors inside shock wave zone and associated flow field is difficult. Across the shock wave, the pressure and density of the fluid change at extremely high rates, which affect the light refraction. The intensity of the Schlieren light is a function of the medium density, which is a function of the light ray path position. The contrast of each pixel is determined by analyzing the image. The equations of Schlieren intensity light are derivated to be a function of Mach number. These functions are applied on an image of shockwave around hemisphere-cylinder at M=1.96.

To verify the results two-dimensional Navier-Stokes equations and conservation

Accepted March 23, 2003.

of energy equation are used to model the flow field and determine Mach number distribution around a hemisphere-cylinder of the supersonic flow, shock waves and associated flow field at the same previous conditions. The governing equations are discretized on a structured grid using an upwind difference scheme. The computational and experimental results show that there is a good matching in the iso-contour of the Mach number with difference less than 3%. The new proposed technique successfully represents the upstream region, the shock wave region, the subsonic region and the expansion fan region. This difference may be due to the noise in the image. This noise can be eliminated if Schlieren light received directly on a CCD camera. The results show that this analysis can be applied for both bright and dark regions of the Schlieren image with correcting the phase shift in the dark area. This optical technique has the advantages of optical measurements. This optical technique has all the advantages of optical measurements as does not disturb the flow and the high sensitivity to capture rapid variation.

KEYWORDS

Image analysis, Schlieren, Supersonic, High subsonic, CFD.

NOMENCLATURE

a_o, b_o	dimensions of light at conjugate focus	m
a_s, b_s	dimensions of light source	m
c_0	speed of light	m/s
C	Gladstone-Dale constant	
C_1, C_2, C_3	constants	
f_1, f_2	focal length of lens	m
I_d	illumination at a position x, y of the image of disturbed field with knife-edge	
I_k	illumination at a position x, y of the image of undisturbed field with knife-edge	
I_o	illumination at a position x, y of the image without knife-edge	
k	the ratio of specific heats	
L, L_1, L_2	the focus lenses	m
M	Mach number	
n	index of refraction of a homogeneous transparent medium	
ΔZ	deviation distance	m

GREEK LETTERS

α	ray deflection angle in air outside test section	degree
α'	ray deflection angle in air without test section	degree
β	Angle defined in Fig. 2	degree
δ	turning flow angle across shockwave	degree
ρ	density	kg/m^3
σ	angle of shockwave to incoming flow	degree
$\Delta\tau$	interval time	s

SUFFIXES

a	ambient air outside test section
e	element
o	standard condition
s	stagnation

Sr source

1. INTRODUCTION

The Schlieren technique is a well-known optical method that depends on the variation of the index of refraction in a transparent medium, Schlichting (1968). Schlieren system is set to indicate variations in the first derivative (normal to the light beam) of the index of refraction. Boundary layers were observed by many authors in air and water or with liquid jet injection, Johnson and Sreenivasan (1993). Schlieren images have also been used to quantify density variations. The relation between density gradients and refraction index is presented according to Lorenz – Lorentz relation.

$$\frac{1}{\rho}\frac{n^2-1}{n^2+2}=const \qquad (1)$$

when $n \cong 1$, this reduces to the Gladstone-Dale equation, Goldstein (1996).

$$\frac{n-1}{\rho}=C \qquad (2)$$

which holds quite well for gases. The constant C, called the Gladstone-Dale constant. It is a function of the particular gas and varies slightly with wavelength. The first derivative (with respect to y) relative to standard condition is determined as.

$$\frac{\partial \rho}{\partial y}=\frac{1}{C}\frac{\partial n}{\partial y}=\frac{\rho_0}{n_0-1}\frac{\partial n}{\partial y} \qquad (3)$$

The relation between the refraction angle and the gradient of the refraction index in an inhomogeneous medium is demonstrated in Fig. 1. Index of refraction varies (for simplicity) only in the y direction. The local value of the speed of light is c_o/n. Two rays in the beam will travel different distances according to the schematic drawing in Fig. 1. It is assuming that only small deviation occurs, the distance ΔZ that the light beam travels during time interval $\Delta\tau$ is:

$$\Delta Z = c_o \,.\, \Delta\tau / n \qquad (4)$$

$$\Delta^2 Z = \Delta Z_y - \Delta Z_{y+\Delta y} = -\frac{\Delta(\Delta Z)}{\Delta y}\Delta y \qquad (5\text{-a})$$

or

$$\Delta^2 Z = -c_0 \frac{\Delta(1/n)}{\Delta y}\Delta\tau.\Delta y \qquad (5\text{-b})$$

The angular deflection of the ray is

$$\Delta\alpha' \approx \frac{\Delta^2 Z}{\Delta y} = -n\frac{\Delta(1/n)}{\Delta y}\Delta Z \qquad (6)$$

In the limit, Δy and ΔZ are considered very small or small deflections. If the entering angle is zero, the exit angle of the test region is

$$\alpha' = \int \frac{1}{n}\frac{\partial n}{\partial y}dz = \int \frac{\partial(\ln n)}{\partial y}dz \qquad (7)$$

If the test region is enclosed by glass walls and the index of refraction within the test section is different from that of the ambient air n_a, then from Snell's law, an additional

angular deflection is present. If α is the angle of the light beam after it has passed through the test section and emerged into the surrounding air,

$$n_a \sin\alpha = n \sin\alpha' \tag{8}$$

$$\alpha = \frac{1}{n_a}\int \frac{\partial n}{\partial y} dz \tag{9}$$

Since $n_a \cong 1$

$$\alpha = \int \frac{\partial n}{\partial y} dz \tag{10}$$

The Schlieren system is basically a device to measure or indicate the refraction angle α, typically of the order of 10^{-6}-10^{-3} rad, as a function of position in the xy plane normal to the light beam. A schematic of the system is shown in Fig. 2. It consists of a light source, which is generally assumed to be rectangular (of dimensions a_{sr}, by b_{sr}) and at the focus of lens L_1. It provides a parallel light beam entering the field of disturbance in the test section. Crosshatched lines indicate the deflected rays, when disturbance is present. A second lens L_2, at its focus a knife edge is placed, collects the light. The light then passes onto a screen located at the conjugate focus of the lens. If no disturbance is present, the light beam at the focus of L_2, would be as shown in Fig. 3, with dimensions a_o by b_o, which are related to the initial dimensions by

$$\frac{a_0}{a_{sr}} = \frac{b_0}{b_{sr}} = \frac{f_2}{f_1} \tag{11}$$

The knife-edge should be adjusted, when no disturbance is present, that $a_k=a_o/2$. The illumination at the screen when no knife-edge is present is I_o, and with the knife-edge is inserted in the focal plane, the illumination is

$$I_k = \frac{a_k}{a_o} I_0 \tag{12}$$

If the light beam at a position x, y in the test region is deflected by an angle α, then from Fig. 2, the image of the source coming from that position will be shifted at the knife-edge by an amount

$$\Delta a = \pm f_2 \alpha \tag{13}$$

where the sign is determined by the orientation of the knife-edge; it is positive when $\alpha > 0$ gives $\Delta a > 0$, and negative if the knife-edge is reversed, so that $\alpha < 0$ leads to $\Delta a < 0$. From Fig. 2 and 3 the illumination at the image of position x, y on the screen will be

$$I_d = I_k \frac{a_k + \Delta a}{a_k} = I_k\left(1 + \frac{\Delta a}{a_k}\right) \tag{14}$$

Where Δa is positive if the light is deflected away from the knife-edge, and negative if the light is deflected toward the knife-edge. The relative intensity or contrast is

$$contrast = \frac{\Delta I}{I_k} = \frac{I_d - I_k}{I_k} = \frac{\Delta a}{a_k} = \pm \frac{\alpha f_2}{a_k} \tag{15}$$

Combining Eqns. (9) and (15), one obtains

$$Contrast = \frac{\Delta I}{I_k} = \pm \frac{f_2}{a_k n_a} \int \frac{\partial n}{\partial y} dz \tag{16}$$

Assuming a two-dimensional flow field with $\partial n/\partial y$ constant at given x, y position over the length L in the z direction

$$Contrast = \frac{\Delta I}{I_k} = \pm \frac{f_2}{a_k n_o} \frac{\partial n}{\partial y} L \qquad (17)$$

If the deflection is toward the knife-edge, the field will darken and the contrast will be negative. It will be positive if y<0. For a gas, Eqn. (17) can be rewritten using Eqn. (3).

$$\frac{\Delta I}{I_k} = \pm \frac{f_2}{a_k n_o} \frac{n_0 - 1}{\rho_0} \frac{\partial \rho}{\partial y} L \qquad (18)$$

when $n_o \cong 1$

$$\frac{\Delta I}{I_k} \cong \pm \frac{f_2}{a_k} \frac{n_0 - 1}{\rho_0} \frac{\partial \rho}{\partial y} L \qquad (19)$$

Turnbull et al (1993) developed quantitative laser Schlieren technique to measure the change in neutral gas density inside a spark gap switch after break down. In another application Zanelli et al (1993) used quantitative Schlieren of the beam forming for therapy with high intensity focused ultrasound. Another variation of Schlieren flow visualization a tricolored filter pattern made up of concentric rings is used instead of a knife-edge at the cut-off plane. Oren and et al (1988) used this method to examine both premixed and diffusion flames in an unsteady swirling flow within a cylinder.

Quantitative visualization of the images of cold swirl jet flow was presented by, Mostafa et al (1996). The non-reacting jet flow field structure was determined from gray scale images of a laser sheet light scattered by smoke particles introduced into the main jet. Because the light intensity is a measure of the dispersion of fluid from the jet (nozzle fluid), it is a measure of mass transfer. Mostafa and Vandsburger (1998) applied quantitative flow visualization to determine jet flame structure and mixing regions. In this application, the light contrast from color images was used to set iso-intensity contour maps of the flame chemiluminescence and soot luminosity regions.

In the present research, a 2D analysis for computing the Mach number distribution in a flow field using Schlieren images across a shock wave in supersonic and high subsonic are described. Quantitative Schlieren images in each pixel are used to provide the level of light beam intensity. The equations of Schlieren intensity light are derivated to be function of Mach number. The present proposed technique was applied determine the velocities flow field using Schlieren image of shockwave around a hemisphere-cylinder at M=1.96, Van Dyke (1982). For verifying the results a 2D numerical computation with Navier-Stokes equations and conservation of energy equation are used to model the supersonic flow, shock waves and associated flow field at the same previous conditions. The governing equations are discretized on a structured grid using an upwind difference scheme.

2. THEORETICAL APPROACH

Across the shock wave, the pressure and density of the fluid change at extremely high rates. These rates are so high that they significantly affect the light refraction. The intensity of the Schlieren light is a function of the medium density, which is a function of the light ray contrast. By integrating Eqn. 18 along an element in the y direction,

assuming that the variation is only in y direction, the contrast over one element ($\Delta I_e/I_k$) will be

$$\frac{\Delta I_e}{I_k} \cong \pm \frac{f_2}{a_k n_a} \frac{n_0 - 1}{\rho_0} \rho_e L + C_1 \qquad (20)$$

where C_1 is a shift of contrast depending upon the method of digitizing the picture. By normalizing the image to the highest light contrast ratio, then

$$\frac{\Delta I_e}{I_k}\Big|_n \cong \pm \frac{C_2 f_2}{a_k n_a} \frac{n_0 - 1}{\rho_0} \rho_e L \qquad (21)$$

where C_2 is a constant.

For an isentropic process in an ideal gas, the density at any element, ρ_e, is related to the stagnation density, ρ_S, and Mach number, M, with the following relation

$$\rho_e = \rho_S \left(1 + \frac{k-1}{2} M^2\right)^{-1/k-1} \qquad (22)$$

Combining Eqns. 21 and 22 gives a relation between the normalized light intensity ratio and Mach number.

$$\frac{\Delta Ie}{I_k}\Big|_n \cong \pm \frac{C_2 f_2}{a_k n_a} \frac{n_0 - 1}{\rho_0} l \rho_S (1 + \frac{k-1}{2} M^2)^{-1/k-1} \qquad (23)$$

then

$$\frac{\Delta Ie}{I_k}\Big|_n \cong \pm C_3 (1 + \frac{k-1}{2} M^2)^{-1/k-1} \qquad (24)$$

where $C_3 \cong \pm \frac{f_2}{a_k n_a} \frac{n_0 - 1}{\rho_0} l . \rho_S . C_2$ (25)

To relate the corresponding image to Mach number, the image is divided to pixels. The image is read pixel by pixel. The contrast at each pixel is determined. Each group of pixels is then binded to create elements or "super pixels", which represent an integrated area. The binding increases the signal to noise ratio at the expense of spatial resolution. A normalized light intensity ratio $[\Delta I_e/I_k]_n$ is then obtained relative to the maximum light intensity. At least one initial condition is needed at each region (upstream region) in order to determine C_3. The local Mach number can be computed at each element in the domain. In case of oblique shock wave the stagnation density changes after the shock waves, so, it is needed to determine the Mach number just after the shock wave from the shock relations, M_2, (Shapiro, 1953).

$$M_2^2 \sin^2(\sigma - \delta) = \frac{1 + \frac{k-1}{2} M_1^2 \sin^2 \sigma}{k M_1^2 \sin^2 \sigma - \frac{k-1}{2}} \qquad (26)$$

where σ angle of shock wave to incoming flow. The turning flow angle across shock δ has a relation with σ and the upstream Mach number before the shock wave, M_1.

$$\tan \delta = \frac{M_1^2 \sin 2\sigma - 2 \cot \sigma}{M_1^2 (k + \cos 2\sigma) + 2} \qquad (27)$$

From Eqns. (26) and (27) Mach number just after the shock wave can be calculated as a function of the upstream Mach number, M_1, and the shock angles across each horizontal

element. Assuming constant stagnation density in the horizontal direction after the shock wave, Eqn. (24) can be used to determine the local Mach number in each element at the expansion zone.

3- Grid Structure and Boundary Conditions For Numerical Solution

To verify the results of 2D Schlieren light analysis, two-dimensional Navier-Stokes equations and conservation of energy equation are used to model the flow field around a hemisphere-cylinder for the supersonic flow, shock waves and associated flow using CFDRC, (2000). The governing equations are discretized on a structured grid using an upwind difference scheme. The structure grids are symmetry around X- axis. The symmetrical half of the structure grids are divided into three blocks around the hemisphere-cylinder each have about 80x50 grid points as shown in Fig. 4. The total number of cells is 8910. This uses the multiblock system. The grids are clustered near the body to solve the fluid interaction. The length of the grid in physical domain is about sixteen of cylinder diameter. The upstream boundary conditions are at Mach number 1.96 and the temperature is 300 K. The downstream boundary conditions are atmospheric pressure. Fluids in all blocks are completely air.

4- Results And Discussion

In this quantitative study, the standard Schlieren images are analyzed to determine the normalized contrast intensity ratio. The Mach number is computed as a function of density and the normalized contrast intensity ratio.

Figure 5 shows Schlieren image of a hemisphere-cylinder at M=1.96 which was obtained by Van Dyke (1982). The Schlieren knife-edge is horizontal to show the boundary layer on the cylinder. The Reynolds number is 82,000 based on nose radius. There is no evidence of separation at the sphere-cylinder juncture. Two windows are selected, one in the bright region and one in the dark region as shown by the dotted lines in Fig. 5. These two images are digitized and analyzed in Figs. 6 and 7. These figures show the normalized contrast intensity ratio integrated over 8x8 pixels area. The comparison between these two figures indicates that there is a phase shift change due to knife-edge and light source position.

From upstream Mach number before the shock wave and the normalized contrast intensity ratio the constant, C_3, is determined from Eqn. 24. Assuming constant stagnation density at each horizontal line before the shock wave, the constant, C_3 has the same value before the shock wave at these elements. By using the local normalized contrast intensity ratio, after removing the phase shift, the Mach number at each element of the domain before shockwave is determined and shown in Figs. 8, 9. The Mach number just after the shock wave can be determined from the upstream Mach number and the shock wave angles, which determined from the shock relations, Eqns. 26, and 27. From the Mach number after the shock wave with the normalized contrast intensity ratio the constant, C_3, is determined at each horizontal line. Assuming constant stagnation density in the horizontal direction after the shock wave, Eqn. (24) can be used to determine the local Mach number in each element at the expansion zone. By using the local normalized contrast intensity ratio, after removing the phase shift, the Mach number at each element of the domain is determined and shown in Fig. 8 for the upper half of the hemisphere cylinder. Figure 9 represents the Mach number distribution of the lower half of the

hemisphere cylinder. These two figures successfully represent the upstream region, the shock wave region, the subsonic region and the expansion fan region. It is clear that there is re-expansion after the shock wave. Figures 8 and 9 are approximately similar due to the symmetry of the hemisphere cylinder. The values of the Mach number after the shock waves are not identical after the shock wave in both sides. This may be due to noise in the lower part image even upstream of the shock as shown in Fig. 5.

To verify the results two-dimensional Navier-Stokes equation and conservation of energy equation are used to model the flow field and determine Mach number distribution around hemisphere-cylinder of the supersonic flow, shock waves and associated flow field at the same previous conditions.

Figures 10, 11, 12 and 13 demonstrate the numerical results of pressure, total pressure, temperature and density contours, respectively, around a hemisphere sheet with the same upstream condition. The iso-contours of pressure, temperature and density have the same trend of the shape of shock wave. The total pressure has the same trend around the nose only. Figure 14 demonstrates the numerical results of Mach number contours around a hemisphere sheet with the same upstream condition. It gives the same previous distribution of, the shock wave region, the subsonic region and the expansion fan region, which were in the image analysis results. The computational and experimental results show that there is a good matching in the iso-contour of the Mach number shown in Figs.9 and 14. The difference between image analysis and numerical computational results is due to a noise in the image. The difference between them is up to 3%. This noise can be eliminated if Schlieren light received directly on a CCD camera. Thus, the image analysis technique is successfully represents the upstream region, the shock wave region, the subsonic region and the expansion fan region.

5- Conclusion

This technique uses the standard Schlieren image successfully to compute the local Mach number. The technique successfully represents the upstream region, the shock wave region, the subsonic region and the expansion fan region. The proposed technique for obtaining flow field from Schlieren flow visualization is valid for both bright and dark regions with correction of the phase shift in the dark area.

The two-dimensional Navier-Stokes equations and conservation of energy equation are modeled the flow field and determined Mach number distribution around hemisphere-cylinder of the supersonic flow, shock waves and associated flow field for the same previous conditions.

The computational and experimental results show that there is a good matching in the iso-contour of the Mach number. The difference between image analysis and numerical computational results may be due to a noise in the image. The difference between them is less than to 3%. This noise can be eliminated if Schlieren light received directly on a CCD camera. This optical technique has all the advantages of optical measurements as the absence of an instrument probe, especially in this application of shock wave. The light beam can also be considered inertialess, so that very rapid transitions can be captured. The technique is simple for computing the velocity in the domain of shock wave and expansion zones.

6- References

CFDRC, 2000, "CFD-ACE+ Theory And Users' Manuals Ver.6.4" *CFD Research Corporation*, Huntisville, Al., USA.

Goldstein, R. J., 1996, "Fluid Mechanics Measurements", *Taylor & Francis Publishers*, chapter seven, Goldestin, R. J. and Kuehn, T. H. "Optical System For Flow Measurement: Shadowgraph, Schlieren, and Interfermetric Techniques", PP 451-471.

Johnson, A. W. and Sreenivasan, K. R., 1993, "Observations Of Liquid Jets Injected Into A High Accelerated Supersonic Boundary Layer" *AIAA Journal,* Vol. 31, No. 10, PP. 1827-1834.

Jr, H. O., 1991, "Optical Measuring Techniques" *Experimental Heat Transfer, Fluid Mechanics, and Thermodynamics*. PP. 290-295

Mostafa, N. H., Vandsburger, U., and Economides, T.A., 1996, "Flow Field Characteristics of a Turbulent Round Jet Subjected to Pulsed Vortex Generating Jets" *ASME Fluids Engineering Division Summer Meeting* , FED-Vol. 237, PP. 535-542. High Speed Jet Flows Forum, San Diego, CA USA, July 7-11.

Mostafa, N. H.and Vandsburger, U.,1998, "The Visible Structure of Turbulent Jet Flames Subjected to Vortex Generating jets" *ASME Fluids Engineering Division Summer Meeting, High Speed Jet Flows Forum,* Washington D.C., USA, June 21-25,.

Oren, D. C., Durrett, R. P., and Freguson, C. R., 1988, "Bullseye Color Schlieren Flow Visualization" *J. Experiments in fluids*. Vol. 6. PP. 357-364.

Schlichting , H., 1968, "Boundary- Layer Theory" *Mc Graw Hill*, 6 Th. edition. Vol. XIII " Laminar Boundary Layer In Compressible Flow/Interaction Between Shock Wave And Boundary Layer"" PP 346-361.

Shapiro, A. H., 1953 "The Dynamics And Thermodynamics Of Compressible Fluid Flow" *New York, Ronald Press Co.*, Vol. 1, PP 532-539.

Turnbull, S. M., MacGregor, S.J., Tuema, F. A., Farish, O., 1993, "A Quantitative Laser Schlieren Method For Measurement Of Neutral Gas Density In High-Pressure Gas Switches" *Meas. Sci. Technol*. Vol. 4. PP. 1154-1159.

Van Dyke, M., 1982, "An Album Of Fluid Motion" The Parabolic Press, Stanford, California, Fig. 267.

Zanelli, C. I., DeMarta, S., Hennige, C. W., and Kadri, M.M., 1993, "Beamforming For Therapy With High Intensity Focused Ultrasound (HIFU) Using Quantitative Schlieren" *Ultrasonics symposium – IEEE*. PP. 1233-1238.

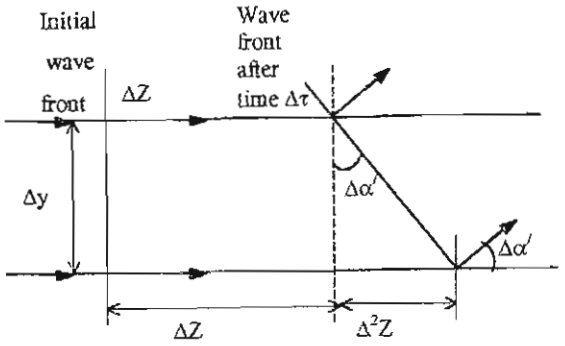

Fig. (1) Bending of light rays in an inhomogeneous medium.

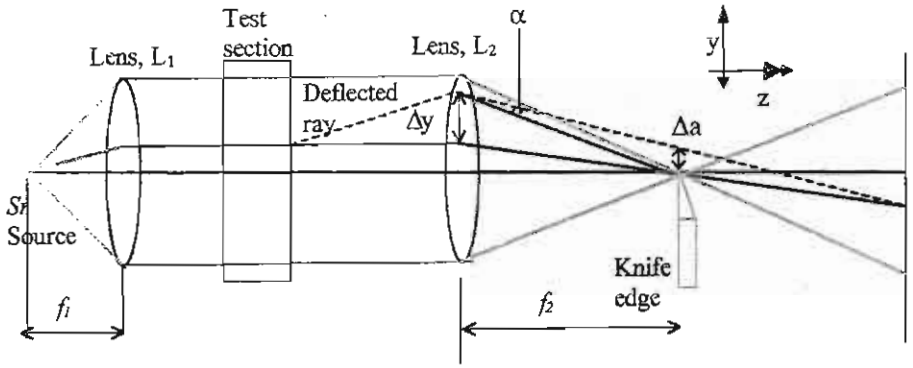

Fig. 2 Typical Schlieren system using lenses.

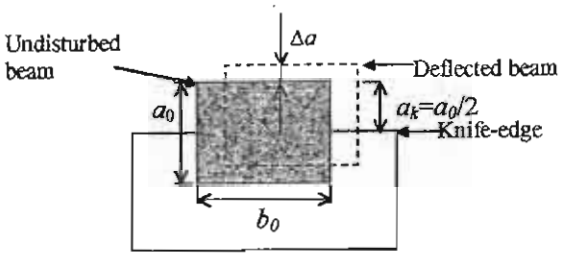

Fig. 3 View of deflected and undisturbed beams at the knife-edge.

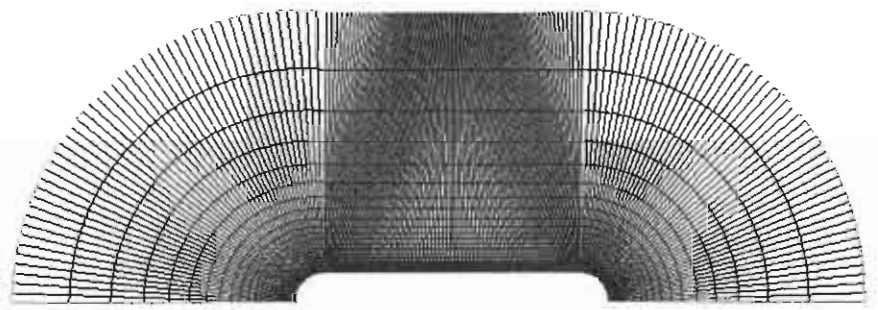

Fig. (4) 2D symmetrical structure grid.

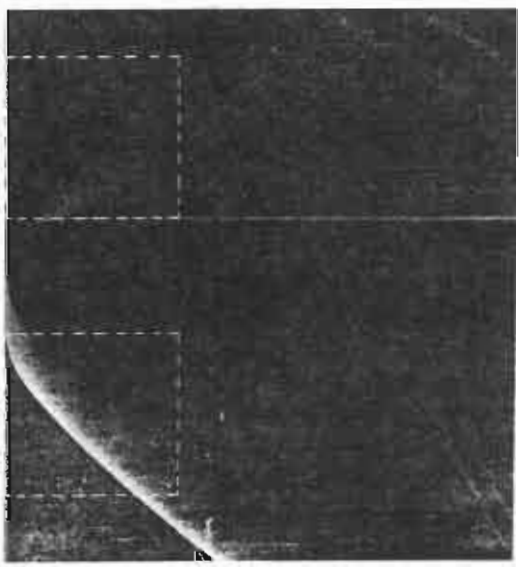

Fig. 5 Schlieren image of hemisphere-cylinder at M=1.96 (Van Dyke, 1982).

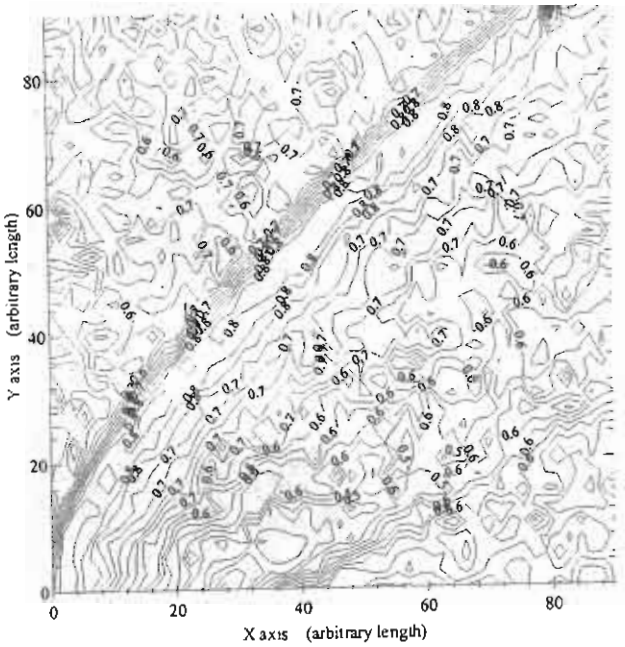

Fig. 6 Normalized contrast intensity at the upper side of the hemisphere-cylinder.

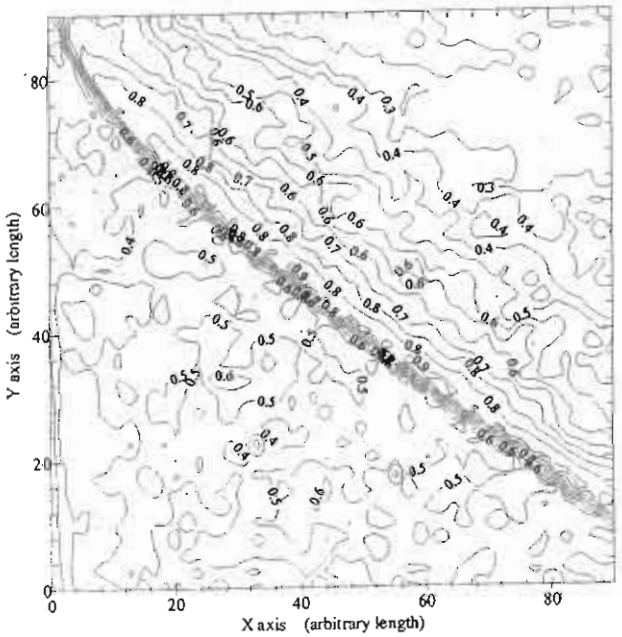

Fig. 7 Normalized contrast intensity at the lower side of the hemisphere-cylinder.

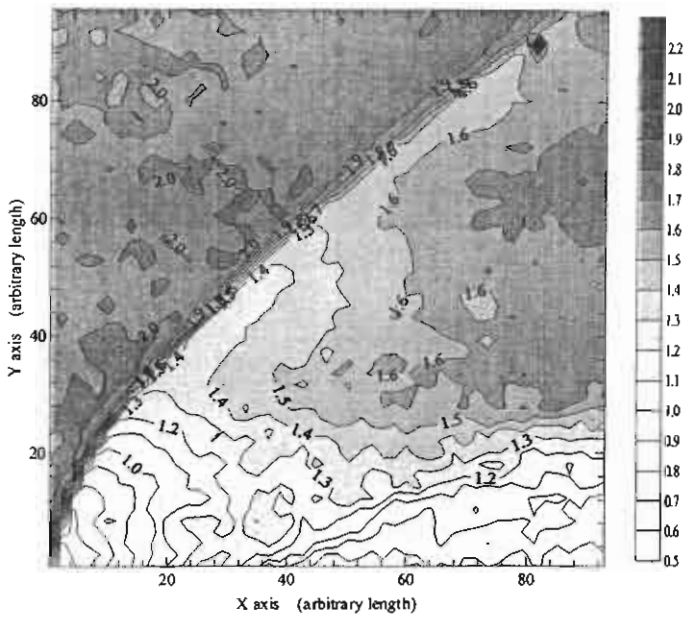

Fig. 8 Mach number at the upper side of the hemisphere-cylinder.

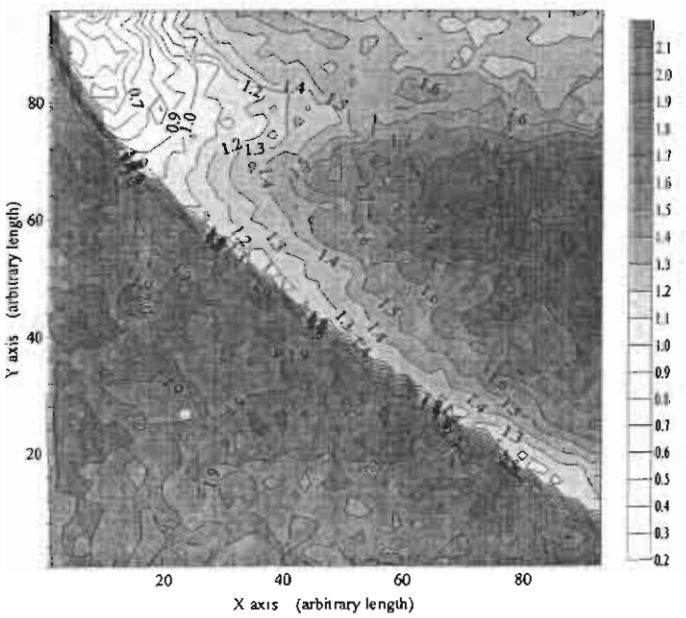

Fig. 9 Mach number at the lower side of the hemisphere-cylinder.

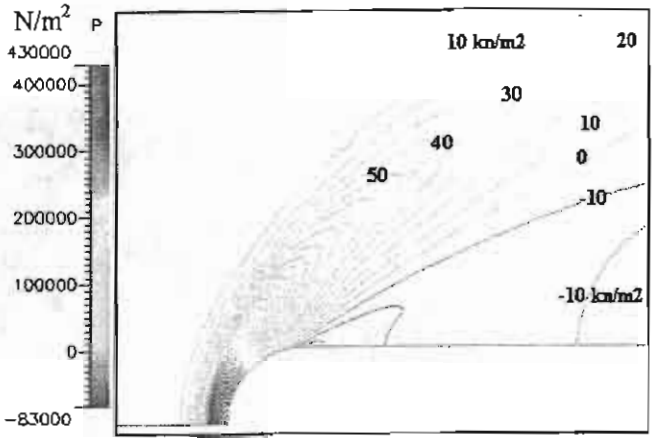

Fig. 10 Numerical pressure distribution at the upper side of the hemisphere-sheet.

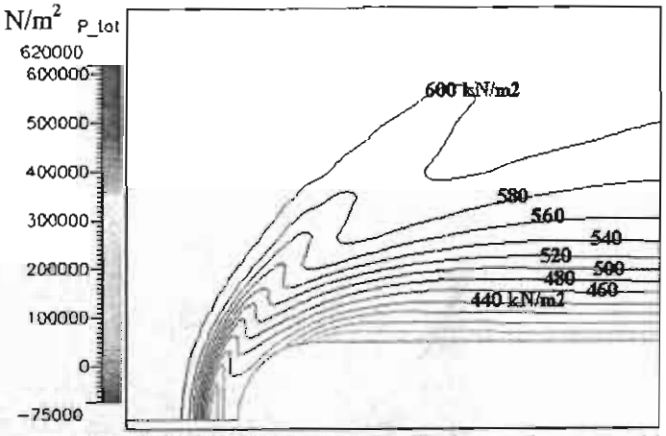

Fig. 11 Numerical total pressure distribution at the upper side of the hemisphere-sheet.

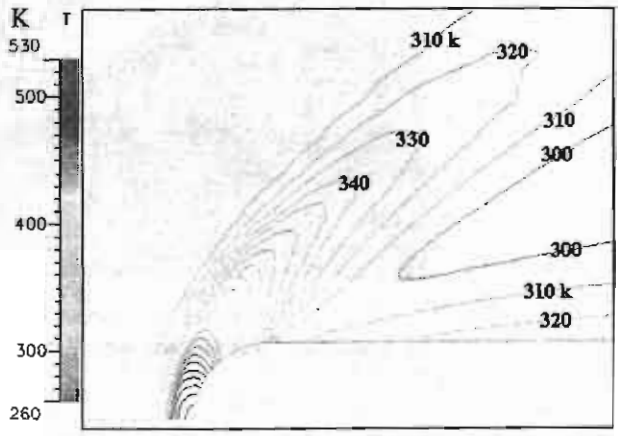

Fig. 12 Numerical temperature distribution at the upper side of the hemisphere-sheet.

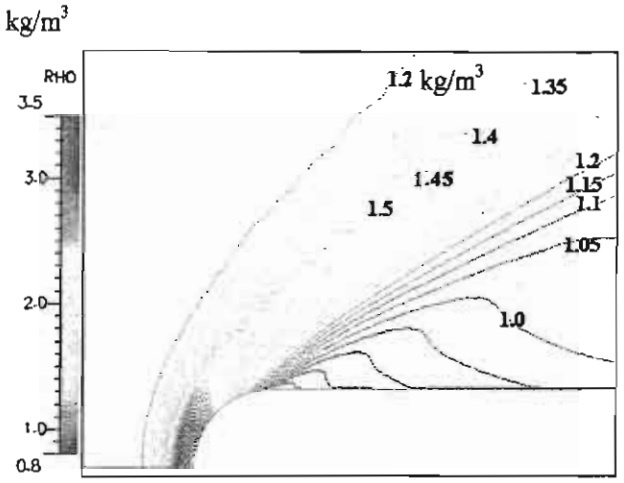

Fig. 13 Numerical density distribution at the upper side of the hemisphere-sheet.

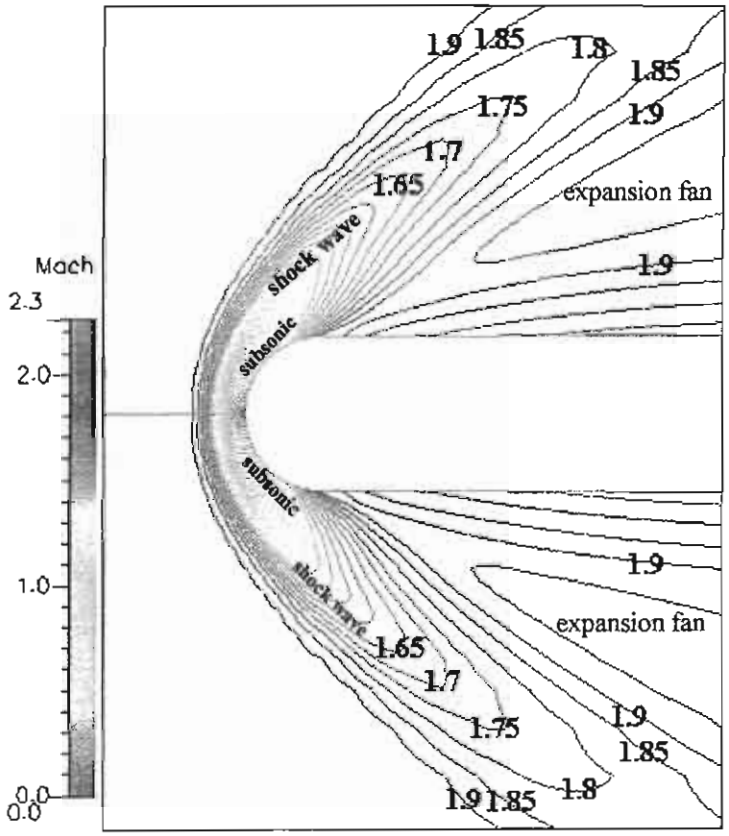

Fig. 14 Numerical Mach number distribution around the hemisphere-sheet.